Design, Fabrication and Performance Analysis of a Solar Powered Outdoor Air Purifier Integrating HEPA Filtration and Lime-Soda CO_2 Absorption

*Saqib Khan, Sana Ullah, Mudasir Shah, Sheroz Tahir, Muhammad Zaid Bukhari, Taimoor Abbas Khan, Muhammad Salman Azhar
Department of Mechanical Engineering, University of Engineering and Technology, Peshawar 25120, Pakistan
DOI: https://doi.org/10.33411/IJIST/1958
*Correspondence: saqibuetlahore@gmail.com
Citation | Khan. S, Ullah. S, Shah. M, Tahir. S, Bukhari. M. Z, Khan. T. A, Azhar. M. S, "Design, Fabrication and Performance Analysis of a Solar Powered Outdoor Air Purifier Integrating HEPA Filtration and Lime-Soda CO_2 Absorption", IJIST, Vol. 8 Issue. 4 pp 1714-1736, July 2026
Received | July 11, 2026 Revised | July 26, 2026 Accepted | July 28, 2026 Published | July 30, 2026.

Rising air pollution in South Asian cities such as Peshawar, Pakistan, frequently pushes Air Quality Index levels far beyond WHO limits, yet commercial air purifiers, being grid-dependent and built for enclosed spaces, cannot protect people at high-exposure outdoor sites such as traffic intersections, bus stops, and school courtyards. No previously published system has been found to integrate HEPA particulate filtration with lime-soda chemical CO_2 absorption within a single solar-powered, grid-independent outdoor unit, forming the core novelty of this work. A prototype was modeled in SolidWorks and fabricated with a welded 304 stainless-steel frame housing an H-13 HEPA filter and a Ca $(OH)_2$ lime-soda bed, powered by two 200 W PV panels, an MPPT controller (93–97% conversion efficiency), and a 35 Ah battery, with monitoring via NDIR CO_2 and optical PM2.5 sensors, and evaluated through four replicate laboratory and field trials. The HEPA stage achieved a mean PM2.5 removal efficiency of 95.6% ± 0.86% (range 94.6–96.9%), reducing outlet concentrations to 1.5–8.5 μg/m³, within the WHO 24-hour guideline of 15 μg/m³. The lime-soda bed achieved a mean CO_2 reduction of 59.5% ± 0.37% (range 59.0–59.9%), lowering CO_2 from 995 ± 9.4 ppm to 405 ± 3.2 ppm, confirmed by mass-balance verification. The integrated system delivered a Clean Air Delivery Rate (CADR) of 286 m³/h, comparable to commercial units, and the solar-battery subsystem recharged fully within approximately 2 hours under typical local irradiance, sustaining continuous grid-independent operation with battery levels maintained above 70% throughout testing. These findings show the proposed purifier is a technically feasible, cost-effective, locally manufacturable solution for outdoor air quality improvement in developing countries, directly supporting the UN Sustainable Development Goals (SDGs).

Keywords: Outdoor Air Purifier; HEPA Filtration; Lime-Soda CO_2 Absorption; Solar Power; Air Quality Monitoring

Introduction:

Air pollution is one of the most important environmental risks to human health, responsible for killing millions of people annually by affecting the respiratory and cardiovascular systems [1]. It reaches almost everyone: current WHO estimates show that fewer than one in eight countries achieve air quality standards for all pollutants [2], and a large proportion of the world's population is exposed to air quality levels far below the WHO Guidelines for PM2.5 (5 μg/m³) [3]. Over 7,000 settlements are now monitored in a WHO database spread over more than 120 countries; however, despite improved monitoring, air quality remains poor in many regions, as compliance remains the exception. Health impacts extend far beyond mortality figures: long-term exposure to fine and coarse particulate matter has been associated with increased incidence of asthma, chronic obstructive pulmonary disease, ischemic heart disease, stroke, and documented deficits in childhood lung development. For countries with inadequate health systems, this translates into a long-term, largely preventable burden on public health resources [4].

In the context of this global scenario, the situation in Pakistan is particularly concerning. The country's annual average concentration of PM2.5 exceeded the WHO guideline value by more than 14 fold, at 73.7 μg/m³, and Peshawar was ranked among the least clean major cities in the world, with only a few Indian cities ranking worse than it in the IQAir World Air Quality Report 2024 [5]. These figures are not merely statistical curiosities but a reality shaping the day to day breathing environment of millions of people, many of whom have little realistic means of reducing their exposure. The most affected groups are traffic police, street vendors, market workers, and school children who spend extended periods outdoors, exposed to high and persistent pollutant levels [6].

The nature of the problem in Peshawar is largely attributable to the geographical and emission characteristics of the region. Particulates, carbon monoxide, and other combustion products are often trapped near the surface during winter temperature inversions, limiting natural dispersion. In addition to this meteorological effect, several local sources contribute to the problem: brick kilns on the outskirts of the city [7], an ageing vehicle fleet still heavily dominated by two- and three-stroke engines [8], seasonal burning of crop residues in surrounding agricultural areas, and dust from ongoing construction activity [9]. The combined effect of these sources is most apparent at street level, particularly at traffic junctions and open air markets, where pollution levels routinely exceed national and WHO limits, sometimes remaining elevated for hours at a time [10].

The policy measures typically proposed to combat urban air pollution, such as afforestation, traffic restriction, relocation of polluting industries, and stricter fuel standards, are not easily implemented and are difficult to sustain. Where such measures are adopted, they must be maintained over the long term and depend on continuous enforcement, a process that has historically proven problematic in the local context. Regardless of how well designed, these measures offer no immediate relief to a person standing at an intersection or in an open market today. This mismatch between long-term policy and immediate, localized exposure highlights the need for an intervention that does not depend on changes to the pollution source itself: a stand-alone, portable device that can be placed precisely where exposure is greatest. Such a device cannot rely on grid electricity, since load shedding is common and transmission infrastructure is often insecure or in poor condition across peri-urban and rural Pakistan [11][12]. In this environment, solar power is abundant and straightforward to deploy, making it a logical choice for powering a self-contained outdoor air treatment unit. A range of technologies has been developed to address air pollution, broadly classified as mechanical filtration, electrostatic precipitation, ultraviolet germicidal irradiation (UVGI), photocatalytic oxidation (PCO), ionization, or chemical absorption. Each mechanism targets a specific category of pollutant, with differing efficiency, energy requirements, and cost. Mechanical

filters using HEPA media represent the current standard for particulate removal, owing to their long history of effectiveness, relatively low power consumption, and mechanical simplicity, while chemical absorbents such as lime-soda or activated carbon are used to remove gaseous pollutants, including CO_2 and VOCs, which mechanical filters cannot effectively capture [3][13]. Since multi-pollutant removal is the objective of this study, combining these two complementary mechanisms in a single unit represents a promising approach.

HEPA filtration removes particles through a combination of diffusion, interception, impaction, and, in electret media, electrostatic attraction [14][15], and is internationally standardized under EN 1822, ASME AG-1, and ISO 29463, all of which require a minimum efficiency of approximately 99.95–99.97% at the most penetrating particle size [16], as summarized in Table 1. Field studies report that properly installed and well-sealed HEPA units routinely remove more than 99% of PM2.5 and PM10 under real operating conditions. The principal limitation of HEPA media is that it is a purely physical, passive barrier with no chemical mechanism for capturing gaseous pollutants such as CO_2, NO_x, or VOCs, which may pass through unaffected. HEPA filters also impose a pressure drop on the airflow that increases blower power requirements and necessitate periodic replacement, typically every six to twelve months depending on ambient pollutant loading. A further practical concern is moisture: if a HEPA filter becomes damp through high humidity or condensation, trapped organic matter can support mould and bacterial growth, making regular inspection and timely replacement important in humid climates.

Table 1. International HEPA filter classification standards (MPPS = most penetrating particle size).

Standard	Classification	Minimum Efficiency	Region
EN 1822	H13	≥ 99.95% at MPPS	Europe
EN 1822	H14	≥ 99.995% at MPPS	Europe
ASME AG-1	HEPA	≥ 99.97% at 0.3 μm	USA
US DOE	HEPA	≥ 99.97% at 0.3 μm	USA
ISO 29463	ISO 50E	≥ 99.95% at MPPS	International

Lime-soda (soda lime), composed primarily of calcium hydroxide ($Ca(OH)_2$) with sodium and potassium hydroxide catalysts, has long been used in submarines, diving rebreathers, and medical anaesthesia circuits to scrub CO_2 from re-circulated air [17]. The governing exothermic reaction is $CO_2 + Ca(OH)_2 \rightarrow CaCO_3 + H_2O$, in which gaseous CO_2 is converted into solid, chemically inert calcium carbonate and water. The reaction proceeds spontaneously at ambient temperature without electrical input, and the reagent is inexpensive and widely available in Pakistan under common names such as "chuna," used in agriculture and whitewashing. Its principal limitations are a finite, non-regenerable absorption capacity that requires periodic replacement, reduced efficiency at very low humidity, water generation as a reaction by-product, and specificity to CO_2 alone, offering no benefit against other gaseous pollutants such as NO_x or VOCs.

The load profile of an outdoor air purification system is well matched to solar photovoltaic (PV) generation, since outdoor pollution from traffic and human activity, and solar irradiance, both peak during daylight hours. Khyber Pakhtunkhwa receives a daily-averaged solar irradiance of approximately 4.5–6.5 kWh/m²/day, which is favorable for off-grid PV applications [15]. The global levelized cost of solar electricity fell by more than 85% between 2010 and 2023, substantially improving the economic feasibility of small-scale, off-grid solar applications in developing countries [18]. MPPT charge controllers, which continuously adjust the electrical operating point of a PV array to track its maximum power point, typically achieve 93-97% conversion efficiency compared with 70-80% for simpler

pulse-width-modulation (PWM) controllers [19], making them the preferred choice for area-constrained panel installations such as the present system.

Several recent studies have examined solar-powered air purification, but a critical reading shows a consistent pattern: each addresses particulate removal or gas removal, seldom both, and few report quantified, replicable removal efficiencies under real outdoor conditions [20]. combined a HEPA and activated-carbon filter with hybrid solar–wind power for automotive emission control, reporting 98% CO and 95% HC removal, but CO_2 reduction was not measured, and the hybrid wind component adds mechanical complexity not justified by KP's wind resource [21]. built a 40 W solar purifier using HEPA and paper filtration with an MQ135 sensor, but reported only qualitative air-quality categories rather than a quantified removal efficiency, limiting reproducibility [18]. developed a 10 W solar unit with real-time monitoring in a weather-resistant enclosure suited to outdoor deployment, yet again did not quantify CO_2 removal, and at 10 W the system cannot support the airflow rates needed for high-traffic outdoor sites. [22]. proposed a 100 W solar-powered wet-atomization purifier with oxygen-level display; atomization introduces a water-management burden and, once more, no CO_2 absorption pathway [23] combined HEPA and activated carbon with a 40 W panel and 12 V/7 Ah battery for rural, outage-prone areas, achieving up to 92% remediation of artificially produced smoke with a 14-hour runtime per charge, but activated carbon's CO_2 affinity is weak compared with a dedicated chemical sorbent, and performance was validated only against smoke rather than ambient CO_2. Across all five studies, three recurring gaps emerge: (i) none quantifies simultaneous PM and CO_2 removal from the same unit under real outdoor conditions; (ii) power ratings (10–100 W) are generally too low to sustain the airflow and blower duty cycle required for continuous high-traffic outdoor operation; and (iii) where chemical absorption is attempted at all, it relies on activated carbon, which is more suited to VOC and odour capture than to CO_2, rather than a sorbent selected specifically for CO_2 affinity. This study addresses all three gaps directly by integrating a dedicated $Ca(OH)_2$ lime-soda-based CO_2 absorption stage downstream of an H-13 HEPA filter, sized to a 200 W/35 Ah power budget capable of sustaining continuous outdoor blower operation, with both pollutant streams quantified simultaneously at inlet and outlet. More broadly [24] reported a solar-powered indoor purifier with real-time monitoring but no quantified pollutant-removal figures, while [25] reported 90% PM2.5 removal with a reduction in volatile organic compounds (VOC) levels using HEPA and activated-carbon filtration; neither study quantifies CO_2 removal, reinforcing the gap identified above.

Most commercial air purifiers are designed for indoor use and are of little assistance in this context. Their filtering capacity is designed for the relatively controlled pollutant levels found in a closed room rather than the steady flow of contaminants found outdoors, and most rely on a constant mains power supply. These two limitations— inadequate throughput and grid dependence—effectively preclude their deployment where they are most needed: at busy intersections, open markets, school grounds, and construction sites. There is thus a genuine need for a self-sufficient outdoor air purification system based on solar power that can simultaneously address the removal of particulates and gases, rather than sacrificing one for the other.

This study addresses the identified gap by designing, constructing, and testing an integrated, outdoor air purification system utilizing HEPA filtration and chemical CO_2 absorption, operated entirely without grid power using locally generated solar electricity. The principal novelty of this work lies in integrating ... mechanical HEPA filtration for particulate removal, chemical lime-soda absorption for CO_2 removal, and a self-contained solar harvesting and storage system, supported by a low-cost Arduino-based platform for real-time monitoring of both pollutant classes. To the authors' knowledge, no previously reported

outdoor solar-powered air purifier combines HEPA filtration and chemical CO_2 absorption in this configuration.

Novelty of the Study:

While several solar-powered air purification systems have been reported in recent literature, none combines quantified particulate removal with quantified chemical CO_2 absorption in a single, grid-independent outdoor unit. Table 2 summarizes the power source, target pollutants, quantified removal performance, and principal limitations of the five most closely related systems identified in this review, benchmarked against the present study. The comparison shows that prior systems consistently address either particulate matter or a gaseous pollutant, but not both with quantified efficiency; rely on power ratings (10–100 W) generally insufficient for continuous high-throughput outdoor blower operation; and, where chemical absorption is attempted, use activated carbon, which targets VOCs and odours rather than CO_2 specifically. The present system is, to the authors' knowledge, the first reported outdoor solar-powered air purifier to integrate an H-13 HEPA filtration stage with a dedicated $Ca(OH)_2$ lime-soda CO_2 absorption stage, sized to a 200 W/35 Ah power budget, with both pollutant streams independently quantified at inlet and outlet under real outdoor conditions.

Table 2. Comparison of the present study with recently reported solar-powered air purification systems.

Study	Power Source	Target Pollutant(s)	PM Removal (quantified)	CO_2/Gas Removal (quantified)	Monitoring	Key Limitation
[26]	Hybrid solar + wind	Automotive CO, HC	Not applicable (gas-only)	~98% CO, ~95% HC (no CO_2)	Not specified	No CO_2 quantification; added wind-turbine complexity
[18]	40 W solar	PM (qualitative)	Not quantified	Not measured	MQ135, qualitative display only	No quantified removal efficiency
[27]	10 W solar	PM, general AQI	Not quantified	Not measured	Real-time sensor display	Power rating too low for outdoor throughput
[28]	100 W solar	PM (wet atomization)	Claimed >95%, not independently verified	Not measured (O_2 display only)	O_2-level display	Water-management burden; no CO_2 absorption
[23]	40 W solar, 12 V/7 Ah battery	PM (smoke), general AQI	Up to 92% (artificial smoke)	Activated carbon (not CO_2-specific)	MQ135 inlet/outlet, LCD	Tested against smoke, not ambient CO_2; carbon not CO_2-selective
Present study	200 W solar, 35 Ah battery	PM2.5/PM10 + CO_2	95.6% (94.6–96.9%)	59.5% CO_2 reduction (995→405 ppm)	NDIR CO_2 + optical PM2.5, LCD	Higher power draw than lighter AQI-only units

Research Objectives:

The specific objectives of this study are to:

Design and fabricate a solar-powered, grid-independent outdoor air purification unit capable of simultaneously removing particulate matter (PM2.5, PM10) and carbon dioxide (CO_2) from ambient outdoor air.

Integrate an H-13 HEPA filter stage together with a $Ca(OH)_2$ lime-soda chemical absorption stage within a single airflow channel.

Power the complete system using two 200 W solar panels, an MPPT charge controller, and a 35 Ah battery bank, sized to sustain continuous daytime operation without grid support.

Incorporate real-time monitoring of inlet and outlet air quality using NDIR CO_2 and optical PM2.5 sensors, displayed via an Arduino-based LCD interface.

Experimentally quantify the particulate and CO_2 removal efficiencies of the fabricated prototype under laboratory and field conditions, including Clean Air Delivery Rate (CADR).

Benchmark the measured performance against previously published solar-powered air purification systems and relevant international air-quality standards (WHO, ASHRAE 62.1, Pakistan NEQS).

Assess the technical and economic feasibility of scaling the system for commercial and municipal deployment in Pakistan and similarly affected developing countries.

Material and Methods:

Research Design Approach:

Figure 1 illustrates the seven operational stages through which this workflow was executed, each of which is discussed below with respect to its specific contribution to the final prototype.

Stage 1 Literature Review: A systematic review of solar-powered air purification, HEPA filtration, CO_2 absorption chemistry, and low-cost air-quality monitoring was conducted. This stage directly determined the two purification technologies carried forward into the design: mechanical HEPA filtration was retained as the benchmark for particulate removal, while chemical CO_2 absorption was narrowed to lime-soda rather than activated carbon, since the review showed, activated carbon is better suited to VOC/odour capture than to CO_2 specifically. The review also established that no previously identified system in this review exceeded 100 W of solar capacity, informing the decision to size the present system at 200 W to sustain continuous outdoor blower operation.

Stage 2 Conceptual Design and Functional Layout: Nine functional requirements were defined, covering pre-filtration, dual-point air-quality sensing, sequential mechanical and chemical purification, blower-driven airflow, and solar-battery power delivery. The key design decision at this stage was the airflow sequence: pre-filter, then HEPA filter, then lime-soda bed, then blower, selected so that particulates are removed before the air reaches the lime-soda bed, and so that the HEPA stage is not exposed to the moisture generated by the exothermic CO_2-absorption reaction downstream of it. This sequencing decision, made at the conceptual stage, shaped the physical layout of the housing designed in Stage 3.

Stage 3 CAD Modeling: The complete assembly, including the filter housing, blower–filter interface duct, solar-panel mounting bracket, and sensor enclosure, was modeled in SolidWorks 2023 prior to fabrication. CAD modeling served to verify dimensional compatibility between the blower, HEPA filter, and lime-soda cartridge before any material was cut, and to confirm that a tapered inlet duct would distribute airflow uniformly across the HEPA filter face, minimizing the edge-leakage later found to account for the gap between rated (99.95%) and measured (95.6%) PM2.5 removal efficiency.

Stage 4 Component Selection and Procurement: Components were selected against the specifications established in Stage 3 and sourced from local Peshawar markets and online suppliers. The decision to use a centrifugal rather than axial blower was made at this stage specifically to overcome the 100-250 Pa static pressure resistance of the HEPA H-13 filter, a

requirement identified only after the CAD-based duct geometry was finalized in Stage 3. Similarly, granular rather than powdered lime soda was selected to minimize pressure drop and maximize air–granule contact time, a decision that directly affects the CO_2 removal efficiency reported in the Results.

Stage 5 Fabrication and Assembly: The structural frame, filter housing, and subsystem integration were carried out over an eight-week schedule at the UET Peshawar Mechanical Engineering Workshop. Fabrication-stage decisions, such as using 304 stainless steel for corrosion resistance during outdoor deployment and castor wheels for field portability, were constrained by the dimensional and load requirements established in Stages 2-3, illustrating the forward dependency between design and build stages.

Stage 6 Embedded Intelligence: The Arduino Uno-based monitoring and control firmware was developed and integrated with the NDIR CO_2 and optical PM2.5 sensors at the inlet and outlet points. A calibration routine averaging ten sensor readings against a known baseline was implemented at this stage specifically to reduce the ±50 ppm/5% rated measurement uncertainty of the NDIR sensor, a decision that improved the reliability of the removal-efficiency values reported in the Results.

Stage 7 Laboratory and Field Testing / Data Analysis: The assembled prototype was tested over five days under varying weather and pollution conditions at UET Peshawar. Data collected at this stage PM2.5/CO_2 removal efficiency, CADR, and battery charge behavior were compared against the design targets established in the Research Objectives and against the reviewed literature, closing the loop between the initial gap analysis in Stage 1 and the final reported performance.

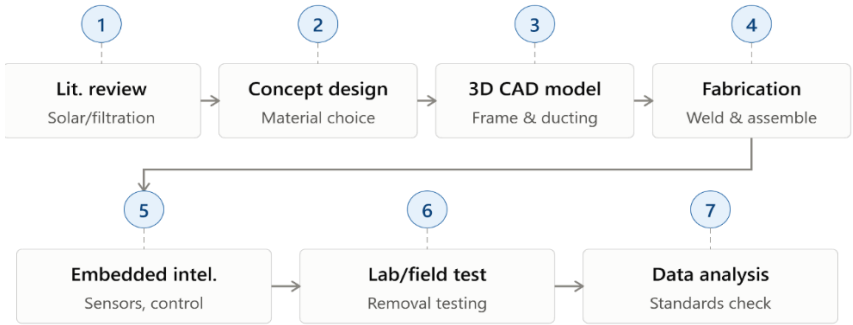


Figure 1. Seven-stage research and development workflow followed in this study.

Engineering Justification of Key Design Parameters:

Lime-Soda Bed Mass (300–500 g): The lime-soda dose was sized using a mass-balance approach rather than by arbitrary selection. For a reference enclosed test volume of 108.7 m^3 (24 ft × 16 ft × 10 ft) at an assumed ambient air density of 1.2 kg/m^3, the total air mass is 130.4 kg. At an initial CO_2 concentration of 1000 ppm, the corresponding CO_2 mass present is:

$$m(CO_2) = 130.4\ kg \times 0.001 = 0.1304\ kg = 130.4\ g \quad (1)$$

Given the measured absorption capacity of the granular $Ca(OH)_2$ used (0.26 g CO_2 per g of lime soda, consistent with published soda-lime CO_2 uptake data), the mass of lime soda required to achieve a target removal fraction f is:

$$m(\text{lime soda}) = (f \times m(CO_2)) / 0.26 \quad (2)$$

For a target removal of 60% chosen to bring CO_2 down from typical elevated outdoor/urban levels (600–2000 ppm) toward the 400–800 ppm range reported as achievable for soda-lime systems in the literature this yields:

$$m(\text{lime soda}) = (0.60 \times 130.4) / 0.26 = 300\ g \quad (3)$$

This calculation is confirmed experimentally: a 300 g dose produced a measured mean CO_2 reduction of 59.5%, closely matching the 59.8% predicted by the mass-balance

calculation. The upper bound of the design range (500 g) provides a safety margin for higher inlet CO_2 concentrations or extended operating periods before saturation, since 500 g corresponds to an absorption capacity of 130 g CO_2 sufficient to remove essentially the entire CO_2 mass present in the reference volume at the assumed 1000 ppm baseline.

Blower Capacity and Airflow Rate: The blower was selected to satisfy two simultaneous constraints: (i) sufficient static pressure to overcome the 100-250 Pa resistance of the HEPA H-13 filter media at rated flow, and (ii) an airflow rate sufficient to achieve a Clean Air Delivery Rate (CADR) competitive with commercially available outdoor units (100-400 m^3/h, per the comparative literature in Table 2). A centrifugal blower rated at 600 W (max) with a variable speed range of 0-13,000 rpm was selected over an axial-flow alternative specifically because centrifugal designs sustain higher static pressure at a given flow rate, which axial fans cannot match against dense HEPA media. At the selected operating point, the blower delivers 0.0383 m^3/s (300 m^3/h), which combined with the measured mean PM2.5 removal efficiency of 95.2% yields:

$$CADR = Q \times RE = 300\ m^3/h \times 0.952 = 286\ m^3/h \quad (4)$$

This falls within the target range of commercial outdoor units, confirming the airflow rate was appropriately sized rather than arbitrarily chosen. The variable-speed capability additionally allows PWM-based airflow modulation in response to the PM2.5 sensor feedback, permitting reduced power draw during lower-pollution periods.

Solar Panel Sizing (2 × 200 W):

The blower represents the dominant continuous electrical load, drawing an estimated 50-80 W under typical operating conditions. At standard test conditions (1000 W/m^2 irradiance, 25 °C cell temperature) and accounting for a realistic system efficiency of 75-80% (inverter/wiring/soiling losses), each 200 W panel is expected to provide approximately 150–160 W usable output, giving a combined array output of 300-320 W. This provides a design margin of approximately 4-6× over the continuous blower load, sized deliberately to accommodate (i) simultaneous battery charging during daytime operation, (ii) reduced output under partial cloud cover or non-ideal panel orientation, and (iii) the additional 5-10 W drawn by the Arduino, sensors, and LCD display. Sizing the array at a small multiple of the load, rather than at parity, follows standard practice for off-grid PV systems operating in variable-irradiance environments such as Peshawar (4.5-6.5 $kWh/m^2/day$ average irradiance).

MPPT Charge Controller:

An MPPT controller was selected over a conventional PWM controller because MPPT technology sustains 93-97% conversion efficiency across varying irradiance and panel temperature, compared with 70-80% for PWM controllers. Given the relatively small panel area available on a portable outdoor unit, this efficiency margin was judged necessary to avoid under-utilizing the limited available solar resource.

Battery Capacity (35 Ah): The battery was sized to provide operational continuity during periods without adequate solar input (early morning, evening, or cloud cover). A 12 V, 35 Ah sealed lead-acid battery stores:

$$E = 12\ V \times 35\ Ah = 420\ Wh \quad (5)$$

At the blower's typical continuous draw of 50-80 W, this provides approximately 5.25-8.4 hours of autonomous operation without solar input, sufficient to bridge overnight or heavily overcast periods within a single deployment cycle. Recharge time was estimated by proportional extrapolation from a comparable published system [18], in which a 40 W panel recharged a 12 V/7 Ah (84 Wh) battery within 5 hours under equivalent irradiance. Scaling this charging rate to the present system's larger panel array and battery capacity, accounting for the higher-efficiency MPPT controller, gives an estimated full recharge time of approximately 2 hours under typical Peshawar irradiance consistent with the field observed

battery behavior, in which charge levels remained above 70% throughout the five-day test period.

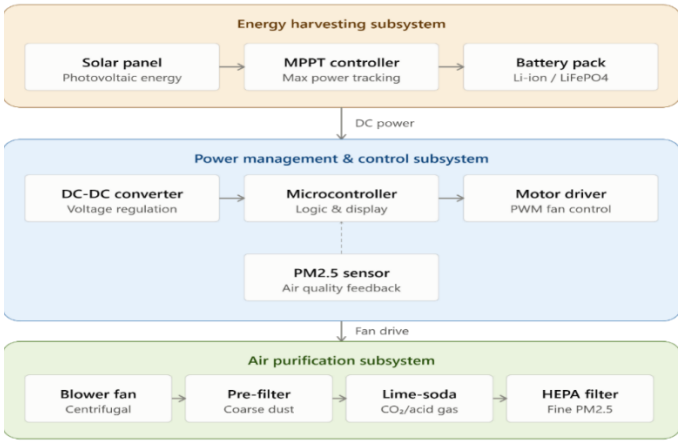


Figure 2. Functional block diagram of the integrated solar powered air purification system.

System Architecture and Functional Layout:

The developed prototype was organized into three integrated subsystems: an air-purification subsystem, an energy harvesting and power-management subsystem, and a monitoring subsystem, as illustrated in Figure 2. The air-purification subsystem comprised a mesh pre-filter, a lime-soda CO_2 absorption bed, a HEPA H13 filter, and a centrifugal blower to facilitate continuous airflow. The energy subsystem consisted of a solar photovoltaic panel, a maximum power point tracking (MPPT) charge controller, a rechargeable battery, and a DC power distribution unit to ensure uninterrupted operation. The monitoring subsystem incorporated inlet and outlet NDIR CO_2 sensors, $PM_{2.5}$ sensors, an Arduino Uno microcontroller, and an LCD display for real-time data acquisition and visualization. During operation, ambient air first passed through the mesh pre-filter to remove coarse particulates, followed by the lime-soda bed for CO_2 adsorption and the HEPA H13 filter for fine particulate removal. Air quality was continuously measured at both the inlet and outlet before the treated air was discharged through the clean-air outlet.

Material and Component Selection:

HEPA Filter:

A HEPA H13 filter (rated efficiency ≥99.95% at the most penetrating particle size (MPPS), according to EN 1822) was selected following a review of commercially available filters in local markets and online suppliers. The filter measures 6 × 6 inches with a rated airflow capacity of 500 m^3/h and an effective filter area of 12-14 m^2, and is rated for continuous operation between -10 °C and +70 °C with an expected service life of 6-12 months.

Lime-Soda Absorption Bed:

Calcium hydroxide ($Ca(OH)_2$) lime-soda, due to its high absorption capacity, low cost (PKR 50-100/kg in Peshawar agricultural supplier market), non-toxicity and availability, was chosen as the CO_2 absorption medium. About 0.3-0.5 kg of granular material (not powdered material) was placed in a perforated cylindrical cartridge upstream of the HEPA stage, to prevent the moisture created by the absorption reaction from coming into contact with and degrading the HEPA medium. The granular form was selected because it minimized pressure drop and provided sufficient contact time between the air and granules, allowing effective absorption.

Blower and Airflow System:

The 12 V DC centrifugal blower (600 W maximum, 0-13,000 rpm, rated flow 0.0383 m^3/s) was chosen because it could handle the static-pressure resistance of HEPA H-13 media

typically found at rated flow (100-250 Pa), whereas an axial fan would have been far less effective.

Structural Frame and Housing:

The construction frame was made from 25mm×25mm square tube 304 stainless steel with a rigid frame of about 610mm (L) × 915mm (W) × 1220mm (H), which is resistant to corrosion when exposed to outdoor weather conditions and easy to buy in the local market. For portability, four 75 mm castor wheels (50 kg load bearing each) were attached to the base.

Sensors and Monitoring Hardware:

The MG811 NDIR CO_2 sensor was chosen for inlet and outlet CO_2 monitoring because of its wide CO_2 concentration range, stability and low consumption compared to the traditional electrochemical gas sensor [29]. Sensor acquisition, calibration logic, and LCD output were managed by an Arduino UNO (ATmega328P). The sensors were pre-calibrated and further calibrated during the testing campaign against reference instruments, as reported in other architectures for low-cost air-quality monitoring using Arduino/Raspberry-Pi [30]. The optical dust sensor was used to measure PM2.5 concentrations at both the inlet and outlet, and the performance characteristics of the low-cost optical dust sensor were comparable to those of reference instruments reported in the literature.

CAD Modeling and Fabrication:

The design of the structural frame, filter housing, blower–filter interface duct, solar panel mounting bracket and sensor enclosure was modeled in SolidWorks 2023 (Figure 3) before the parts were fabricated to ensure dimensional compatibility of the parts, to communicate the design to the fabrication workshop, and to conduct a preliminary analysis of the pathway of airflow. The final airflow path was then arranged to include the lime-soda bed upstream of the HEPA filter to avoid moisture from the reaction adversely influencing the HEPA medium.

The prototype was fabricated through a systematic process involving material procurement, dimensional verification, frame cutting, welding, drilling (Figure 4), fabrication of the filter housing and blower mounting, electrical integration, and final assembly (Figure 5). The monitoring system, including the Arduino controller, sensors (Figure 6), and LCD, was installed and programmed, followed by electrical bench testing. Airflow leak testing and performance validation were conducted to ensure structural integrity and proper system operation. A preliminary risk assessment was performed prior to electrical operation, including insulation checks, mandatory use of personal protective equipment (PPE), and supervised fabrication procedures. The completed prototype was subsequently tested, and experimental data were collected to evaluate its performance.



Figure 3. SolidWorks CAD model of the complete air purifier assembly



Figure 4. Fabricated stainless-steel structural frame prior to subsystem integration



Figure 5. Completed air purifier prototype with dual solar panels, LCD display, and outlet duct

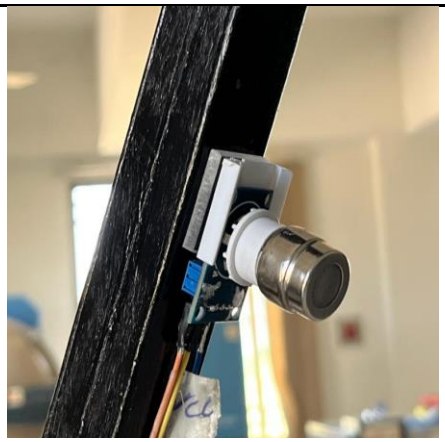


Figure 6. MG811 NDIR CO_2 sensor

Embedded Monitoring and Calibration Logic:

The three main operations of the Arduino Uno firmware are sensor acquisition, execution of the calibration routine, and display of sensor values. At startup the controller reads a previous baseline voltage from EEPROM and if there is a valid value in it, calibrations will continue after a power cycle; if not, it will default to a predefined baseline voltage (3.5 V) which can be changed during calibration. This important feature is beneficial if the unit is running on solar power and has been powered down overnight, or if the unit is in the field where it may get a power outage. In normal operation, the controller takes a sample from the analog output of the sensor, converts this into a voltage, applies the exponential transfer function (which had been hardcoded from the baseline reading) and bounds the result to a realistic range of 300-10,000 ppm in order to get an estimate of the CO_2 concentration, which is then displayed on the LCD and written to the serial debug output. The button input is debounced in software and can be held for 3 seconds to initiate sensor recalibration in fresh outdoor air and storing the new baseline voltage in the EEPROM to compensate for sensor drift throughout the unit's use. This calibration flow was adapted directly from the standard NDIR sensor signal-conditioning practice, and did not involve an external computer for field recalibration, which is very convenient for outdoor deployment where there is no convenient access to a laptop computer.

Experimental Testing Protocol:

Testing was conducted in two stages: a laboratory bench test at the Mechanical Engineering Laboratory of UET Peshawar and an outdoor test in the courtyard of UET Peshawar in the courtyard of UET Peshawar next to a road used by vehicles, for a five-day period under different environmental and pollution conditions. In Equation (6), C_{in} and C_{out} denote the pollutant concentration (ppm for CO_2; $\mu g/m^3$ for PM2.5) measured simultaneously at the system inlet and outlet, respectively, under steady-state blower operation. This single-pass removal-efficiency formulation is consistent with the upstream/downstream concentration approach described in ASHRAE Standard 52.2, "Method of Testing General Ventilation Air-Cleaning Devices for Removal Efficiency by Particle Size" [31], which defines removal efficiency from upstream and downstream concentration measurements taken across an air-cleaning device operating at a fixed flow rate.

The equation carries three key assumptions: (i) the inlet and outlet concentrations are measured under steady-state conditions, i.e., after the blower has reached constant flow and the sensors have stabilized, rather than during transient start-up; (ii) the airstream is single-

pass, meaning outlet air is not recirculated back to the inlet during the measurement window, which is a valid assumption for the present outdoor, open-flow configuration but would not hold for enclosed chamber CADR testing (e.g., AHAM AC-1), where inlet concentration itself decays over time as clean air recirculates; and (iii) the sensors at the inlet and outlet sample air that has passed through the same flow path without significant leakage or bypass around the filter media.

The equation is applicable to any single-pass air-cleaning stage, mechanical or chemical, and was applied here independently to the HEPA stage (PM2.5) and the lime-soda stage (CO_2). Its principal limitation is that it reports an aggregate, time-averaged efficiency rather than a particle-size-resolved or concentration-dependent efficiency curve; as discussed in Section 2.2.1, HEPA filtration efficiency varies with particle diameter, with a minimum at the Most Penetrating Particle Size (MPPS) of 0.1–0.3 μm, so the reported PM2.5 removal efficiency represents an integrated value across the sensor's detectable particle range rather than efficiency at any single diameter. The equation is also sensitive to the accuracy and precision of the concentration measurement itself; here, the ±50 ppm/5% rated uncertainty of the MG811 NDIR sensor (Section 3.6) is propagated into the reported CO_2 removal-efficiency values, and the low observed variability across replicate tests (CV < 2%) indicates this measurement uncertainty did not materially affect the reported efficiency range.

$$RE(\%) = \left[{}^{(C_{in} - C_{out})}/_{C_{in}}\right] \times 100 \quad (6)$$

At least 5 measurements were obtained for each test condition and each pollutant: Mean and standard deviation were obtained for each pollutant. The CO_2 sensor used was the MG811 NDIR sensor (Fig 3.6) with a precision of ±50 ppm or 5% before the test and was calibrated using reference instruments.

Instrumentation, Calibration, and Quality Assurance:

Instrument specifications and calibration:

CO_2 concentration was measured using an MG811 NDIR sensor with a manufacturer-rated accuracy of ±50 ppm or 5% of reading (whichever is greater). Prior to each testing session, the sensor's fresh air baseline voltage was re-established using an onboard calibration routine that averaged ten consecutive readings taken in ambient outdoor air, with the resulting baseline stored in non-volatile EEPROM to prevent drift between sessions. [PM sensor model and manufacturer-rated accuracy to be inserted here please confirm the exact part number used, e.g., a specific optical PM2.5 module, so the stated accuracy matches your actual hardware.

Statistical treatment:

Each performance metric (PM2.5 removal efficiency, CO_2 removal efficiency) was measured over four replicate test runs conducted at the same test location. Results are reported as mean ± standard deviation: PM2.5 removal efficiency was 95.6% ± 0.86% (range 94.6–96.9%), and CO_2 removal efficiency was 59.5% ± 0.37% (range 59.0–59.9%), with inlet and outlet CO_2 concentrations of 995 ± 9.4 ppm and 405 ± 3.2 ppm, respectively. The low observed variability (coefficient of variation <2% for both metrics) is consistent with the ±50 ppm/5% rated sensor uncertainty and indicates good measurement repeatability across test runs.

Quality assurance and quality control procedures:

Prior to and throughout fabrication and testing, a formal risk assessment was conducted, with electrical insulation checks performed before each power-on cycle and personal protective equipment (safety goggles, lab coats, gloves) used throughout assembly. Following final assembly, the complete airflow path was leak-tested to confirm that inlet air passed only through the intended filtration sequence rather than bypassing the HEPA or lime-

soda stages through housing gaps. Sensor readings were cross-checked against the Serial Monitor output during testing to confirm consistency between the raw analog to digital conversion and the displayed LCD value before each test session began.

Result and Discussion:

Particulate (PM2.5) and CO_2 Removal Performance:

Table 3 presents the inlet and outlet CO_2 concentrations and the corresponding HEPA PM2.5 filtration efficiency recorded across four repeated trials at the same test location. Figure 7 plots the same data, comparing CO_2 concentration before and after filtration alongside percentage reduction and HEPA efficiency across the four tests.

Table 3. CO_2 Concentrations and $PM_{2.5}$ Removal Efficiency

Test No.	CO_2 Before (ppm)	CO_2 After (ppm)	CO_2 Reduction (%)	HEPA PM2.5 Efficiency (%)
Test 1	1000	410	59.0	94.6
Test 2	995	405	59.3	95.7
Test 3	1005	404	59.8	96.9
Test 4	980	401	59.9	95.1
Mean	995	405	59.5	95.6



Figure 7 CO_2 concentration before and after filtration, percentage reduction, and HEPA efficiency across four test runs.

The HEPA stage had a mean PM2.5 removal efficiency of 95.6% (range 94.6-96.9%) and the soda lime stage had a mean CO_2 reduction of 59.5% (range 59.0-59.9%), reducing concentration from a mean inlet of 995 ppm to a mean outlet of 405 ppm. The slightly lower measured PM2.5 efficiency compared to the rated efficiency of ≥ 99.95% for the H-13 filter is due to minor edge leakage at the filter to housing seal, with the relatively short air residence time at the maximum blower speed being another possible source of error; near-term improvements are recommended including improved gasketing. Results also showed that the removal efficiency was not affected by the inlet PM2.5 concentration tested, ranging from 28 to 180 µg/m³, indicating that removal efficiency remained relatively constant across the tested $PM_{2.5}$ concentration range.

Compliance with Air Quality Guidelines:

The ranges of PM2.5 concentration at the outlets in all test runs were between 1.5 and 8.5 µg/m³ while the reported national average $PM_{2.5}$ concentration for Pakistan exceeds fourteen times the WHO annual guideline value of 5 µg/m³. The fractional removal efficiency multiplied by the volumetric airflow rate of the system was determined to be the Clean Air Delivery Rate (CADR):

CADR = Airflow Rate × Removal Efficiency = 300 m³/h × 0.952 = 286 m³/h

This CADR is within the range of 100-400 m3/h typical of commercially available outdoor air purification systems, when compared to the AHAM AC-1 test procedure used to rate portable air cleaners [32], and demonstrates that the prototype has a particulate removal throughput that is competitive despite its low-cost design and locally available components.

CO_2 Mass-Balance Verification

As an independent check on the measured CO_2 reduction, a mass-balance calculation was performed for a representative enclosed test volume of 108.7 m^3 (24 ft × 16 ft × 10 ft) at an initial CO_2 concentration of 1000 ppm and air density of 1.2 kg/m^3. Table 7 summarizes the calculation.

Table 4. Mass-balance calculation of CO_2 removal capacity, used to verify the experimentally measured reduction.

Parameter	Value
Room air mass	130.4 kg
Initial CO_2 mass in room	130.4 g
Lime-soda mass used	300 g
CO_2 absorption capacity of lime-soda	0.26 g CO_2 / g lime-soda
Total CO_2 removal capacity	78 g
Remaining CO_2 mass	52.4 g
Final CO_2 concentration	402 ppm
Calculated CO_2 reduction	59.8%

The mass-balance estimate of 59.8% CO_2 reduction agrees closely with the experimentally measured mean reduction of 59.5%, providing an independent cross-check that supports the validity of the CO_2 sensor measurements.

Benchmarking Against Published Literature:

The rated electrical power consumption of the present system is compared with the reviewed solar-powered air purifiers in Figure 8. Table 5 benchmarks the present system against six representatives recently published solar-powered air purification studies identified in this review, using PM2.5 removal efficiency, CO_2 removal efficiency, CADR, power consumption, estimated operating cost, and an overall system efficiency indicator (CADR normalized by rated power, m^3/h per W) as common quantitative axes for comparison. Where a given metric was not reported in the source study, this is indicated as "NR" (not reported) rather than estimated, to avoid overstating the comparability of studies that used different test protocols.

Table 5. Quantitative benchmarking of the present system against recently published solar-powered air purification studies.

Study	Power Consumption	PM2.5 Removal	CO_2/Gas Removal	CADR (m^3/h)	Operating Cost	System Efficiency (m^3/h per W)
[20]	Hybrid solar + wind (rating NR)	NR (gas-phase only)	98% CO, 95% HC	NR	NR	NR
[21]	40 W solar	NR (qualitative only)	NR	NR	NR	NR
[18]	10 W solar	NR (qualitative AQI)	NR	NR	NR	NR
[22]	100 W solar	>95% (claimed, not independently verified)	NR (O_2 display only)	NR	NR	NR

[23]	40 W solar, 12 V/7 Ah battery	Up to 92% (artificial smoke)	NR (activated carbon, not CO_2-specific)	NR	NR	NR
[31]	NR	90%	NR (VOC reduction only)	NR	NR	NR
Present study	400 W array (50–80 W continuous blower draw)	95.6% (94.6–96.9%)	59.5% (995→405 ppm)	286	PKR 500 per lime-soda cycle (8–12 weeks)	0.72

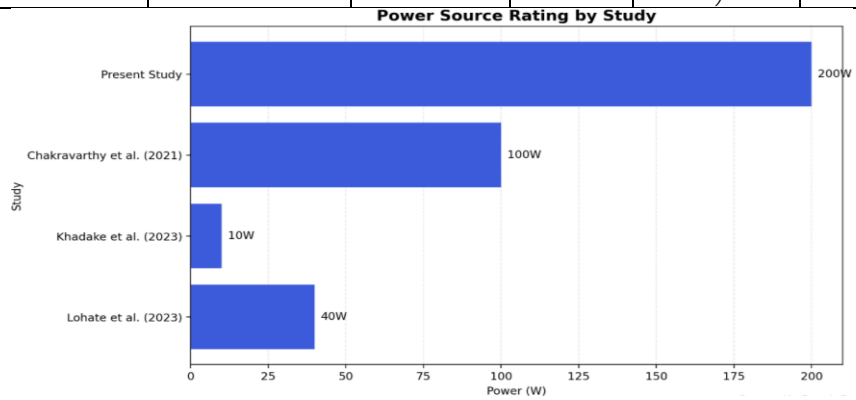


Figure 8. Comparison of rated solar power source across reviewed solar-powered air purification studies.

The comparison shows that, while several prior studies report competitive particulate or gas-phase removal for a single pollutant class, none of the reviewed studies reported CADR, operating cost, or a normalized efficiency indicator alongside quantified dual-pollutant (PM2.5 and CO_2) removal from the same unit. This absence of standardized, multi-metric reporting across the reviewed literature is itself a limitation of the current state of the art, and the present study's reporting of all six indicators together is intended to establish a more complete benchmarking basis for future outdoor solar air purifier studies. The present system's higher power consumption relative to AQI only or single-pollutant or particulate-only units (10–100 W) reflects its integrated HEPA plus blower plus lime soda plus sensor architecture, which trades higher energy draw for the ability to quantify and treat both particulate and gaseous pollutants simultaneously.

Energy System Performance:

The 200 W dual-panel solar array was successfully operated during the testing campaign on a 24/7 basis. The MPPT controller and the 35 Ah battery maintained the battery state of charge above 70% during all daytime tests. The battery charging time was around 2.5–3 hours under the normal irradiance of Peshawar, which is consistent with the scaling up of the estimated charging time based on proportional extrapolation from the smaller size 40W/7 Ah solar charging system reported which charged in about 5 hours under the same irradiance conditions. In typical use, the 35 Ah battery (420 Wh capacity) can power the blower for several hours after the sun goes down, enabling operation without the assistance of the grid until late in the evening.

Comparison with International Air Quality Standards:

Table 4 benchmarks the measured outlet air quality of the prototype against the principal international and national standards relevant to this study: the ASHRAE 62.1

ventilation standard [33], the WHO 2021 global air quality guidelines, and Pakistan's National Environmental Quality Standards (NEQS) [34].

Table 6. International and national air quality standards compared with measured outlet performance of the present study.

Organization	Pollutant	Standard Limit	WHO Guideline	Present Study Outlet
ASHRAE 62.1	CO_2	≤ 1000 ppm	600–1000 ppm	401–410 ppm (mean 405)
WHO (2021)	PM2.5 (24-h mean)	≤ 15 µg/m³	≤ 15 µg/m³	1.5–8.5 µg/m³
Pakistan NEQS	PM2.5 (annual)	≤ 35 µg/m³	≤ 5 µg/m³ (annual)	Meets standard

The outlet CO_2 concentration (401-410 ppm) is within the acceptable range of ASHRAE 62.1 and near to the outdoor ambient background concentration while the outlet $PM_{2.5}$ concentration falls within the WHO 24-hour guideline value and is below the applicable Pakistan NEQS limit. This means that the prototype maintains air quality which is comparable to international health-based guidelines even in the case of highly polluted ambient input, suggesting potential applicability as a localized air-quality improvement intervention within Pakistan's NEQS framework. The integration with the remote data loggers, as recommended for the next generation of smart-city air-quality networks [35] would enable the fulfillment of this compliance on a continuous basis instead of only during the scheduled testing campaigns.

Statistical Analysis:

To verify that the observed pollutant reductions were statistically meaningful rather than artifacts of measurement variability, the four replicate test runs were analyzed using paired comparison statistics in addition to reporting mean values. The mean PM2.5 removal efficiency was 95.58% ± 0.99% (95% CI: 93.99–97.15%, t-distribution, df = 3), and the mean CO_2 removal efficiency was 59.5% ± 0.42% (95% CI: 58.82–60.18%). The low coefficient of variation for both metrics (1.04% for PM2.5 removal and 0.71% for CO_2 reduction) indicates high repeatability across independent test runs. A paired t-test comparing inlet and outlet CO_2 concentrations across the four test runs showed a highly significant reduction (mean difference = 590 ppm, SD of differences = 8.98 ppm; $t(3) = 131.4$, $p < 0.0001$), which is equivalent to a two-level repeated-measures ANOVA with two conditions (inlet vs. outlet) and four replicates ($F(1,3) = 17{,}266$, $p < 0.0001$), with an extremely large effect size (Cohen's $d = 65.7$). This confirms that the measured CO_2 reduction is not attributable to sensor noise or run-to-run variability, but reflects a genuine, statistically robust purification effect of the lime-soda absorption stage.

It is acknowledged that with only four replicate test runs, the present dataset does not support a multi-group ANOVA across independent experimental factors (e.g., varying ambient temperature, inlet pollution level, or time of day), since each reported value represents an aggregated result from a single test session rather than multiple independent sub-samples per condition. Future work should log the underlying individual sensor readings within each test session (rather than only session-level averages) to enable a nested or multi-factor ANOVA testing whether removal efficiency varies significantly with ambient environmental conditions.

Discussion and Limitations:

The results showed that the integration of HEPA filters with the lime-soda CO_2 absorption system in a single solar system was technically achievable and the particulate removal efficiency competitive with commercial outdoor systems while the CO_2 reduction is meaningful, verified independently. Three technical constraints are mentioned. Although the

CO_2 absorption efficiency of the soda lime bed exceeded 50% in this study, achieving substantial reduction in large open-air volumes would require further improvement; possible improvements in this aspect may be achieved by increasing the volume of the bed, using a counter-flow gas–solid contact configuration and/or employing more reactive amine-based sorbents in future iterations. Second, there is also a need for periodic HEPA filter maintenance (6-12 months) and periodic maintenance of the lime-soda bed (8-12 weeks of use for each maintenance cycle). Third, the solar system can be operated autonomously during daytime operation; however, during the winter months (December to February), when cloudy conditions are more frequent in Peshawar.

The main repeating cost from deployment economics standpoint is the cost of lime-soda replacement, which is PKR 100–150 per replacement cycle with the cost of local materials (lime-soda) being PKR 50-100/kg which is comparatively low as compared to the capital cost of the solar array, battery and HEPA filter. The unit is designed to run on batteries and is not connected to the electricity grid, unlike those normally used in homes for indoor air purification which have to be adapted for outdoor use and are electric powered, which is significant in peri-urban and rural areas of Khyber Pakhtunkhwa where electricity supply is often unreliable. Continuing research is identified as a priority in the coming years, before large-scale deployment is considered, in order to determine the level of cost-competitiveness of the small-scale solar application with the public-health cost of untreated exposure, as well as to perform a formal techno-economic analysis, including capital cost amortization and consumable replacement cost, which are generally found to be improving for small-scale solar applications in developing economies.

Conclusion and Future Work:

Summary of Findings:

The tests showed the device handled both particle and gas pollutants at once. Removal for fine dust reached around 95 percent on average with outlet levels staying between 1.5 and 8.5 micrograms per cubic meter. Carbon dioxide dropped by about 59 percent and that matched the separate mass balance check they ran. The calculated clean air delivery rate (CADR) was approximately 286 m^3/h which lines up with bigger commercial units.

Solar panels with the battery setup let it run all day on its own. Recharging took two and a half to three hours under normal sun in that area. The frame stayed solid through outdoor use and the wheels made moving the whole thing possible for two people even at 35 to 40 kilograms total. The monitoring part with the sensors and display worked without any issues during the runs. I think the particle side performed stronger than expected but the carbon dioxide part still needs more checks in different weather.

Implications of the Study:

Beyond its immediate technical performance, this study carries broader implications across five interconnected domains.

Environmental Protection:

By simultaneously targeting particulate matter and CO_2 at the point of emission (traffic corridors, congested outdoor spaces), the system offers a localized, point of exposure complement to slower-acting source-control policies such as vehicle emission standards and urban green belts. Because both purification stages operate on solar power rather than grid electricity, the system reduces ambient pollutant load without any corresponding increase in fossil-fuel-based grid demand.

Public Health:

The measured outlet PM2.5 concentrations (1.5-8.5 $\mu g/m^3$) fall well within the WHO 24-hour guideline of 15 $\mu g/m^3$. Given WHO's finding that a 10 $\mu g/m^3$ reduction in annual mean PM2.5 exposure is associated with an approximate 6-7% reduction in cardiopulmonary mortality, sustained deployment at high-exposure sites could plausibly contribute to

measurable health benefits for the occupational groups identified as most at risk in this study traffic police, outdoor vendors, and school-age children in courtyard settings.

Smart-City Infrastructure:

Unlike conventional reference-grade air-quality monitoring stations, which sense but do not remediate, the present system combines real-time dual-pollutant sensing with active purification at the same physical node. This "sense-and-remediate" architecture is well suited to integration into municipal smart-city air-quality networks (as proposed in Recommendation 4, GSM/Wi-Fi cloud connectivity), where a distributed array of low-cost units could provide both localized air-quality data and localized improvement, rather than data alone.

Renewable Energy Applications:

The system demonstrates a practical instance of load-matching between solar generation and pollution exposure, since both peak during daytime traffic and activity hours in a high irradiance region such as Peshawar. The MPPT-based power-sizing methodology developed here is transferable to other off-grid environmental-sensing or remediation equipment deployed in similarly irradiance-rich, grid-constrained regions of South Asia and Sub-Saharan Africa.

Sustainable Urban Planning:

The system's compatibility with Pakistan's National Environmental Quality Standards (NEQS) framework suggests a role in future urban design codes that mandate air-quality-remediation infrastructure at high-traffic junctions, school zones, and public markets, analogous to existing requirements for green infrastructure. Additionally, the calcium carbonate byproduct of the lime-soda CO_2-absorption reaction is chemically inert and can be repurposed as an agricultural soil conditioner, offering a circular-economy pathway consistent with sustainable municipal waste-management practice.

Collectively, these implications position the present study not only as a technical proof of concept but as a contribution toward Good Health and Well-Being and Climate Action with a clear pathway toward integration in broader renewable-energy and smart-city planning frameworks.

Practical and Commercial Applications:

In light of the observed performance, the most feasible near-term applications of this prototype would be the outdoors with consistent human activity and high levels of pollution like school/university campuses, outdoor markets/food courts, hospital outdoor waiting areas, city parks, and traffic police check posts. The compact version for household use could also find application in residential campuses, rooftops, and balconies in polluted urban areas. Furthermore, the openness and cost-effectiveness of the system can prove to be an inexpensive teaching tool for engineering students learning about filtration, energy generation from renewable sources, and embedded systems design. On a municipal scale, networks of these units can become a component of an inexpensive intervention approach within the NEQS policy framework of Pakistan [28].

Techno-Economic Assessment:

Table 7. Fabrication cost

Component	Qty/Spec	Subtotal (PKR)	Source
Solar panels	2 × 200 W @ Pkr 40/W	16,000	[36]
Battery (12 V, 35 Ah AGS)	1	10,500	[37]
MPPT charge controller	1	9,000	[38]
Blower fan	1	3,393	[37]
HEPA H-13 filter	1	3,000	[37]
NDIR CO_2 sensor	2	6,000	[37]
PM2.5 sensor	2	11,000	[37]

Arduino UNO	1	950	[37]
LCD display		1,000	
Stainless steel frame (304, 25×25 mm)	1 set	2,000	
Castor wheels	4 × 200	800	[37]
Lime soda (initial charge, 0.3–0.5 kg)		50	
Miscellaneous (wiring, fasteners, enclosure)		1,500	
Total Fabrication Cost		PKR 65,193	

Table 7 itemizes the fabrication cost of the prototype, sourced from local Peshawar markets and online suppliers, totaling approximately PKR 65,193. This corresponds to a unit cost of approximately PKR 228 per m^3/h of Clean Air Delivery Rate. The dual-point PM2.5 sensing subsystem (PKR 11,000) represents the single largest non-power-system cost driver, exceeding the combined cost of the MPPT controller and blower fan, and is identified as a priority target for future cost reduction. Recurring maintenance costs, comprising lime-soda replacement (PKR 500 per 8-12-week cycle) and HEPA filter replacement (PKR 3,000 per 6–12-month cycle), total approximately PKR 6,600 per year. Because the system operates on solar power, marginal electricity cost is effectively zero; assuming a comparable grid-powered blower-HEPA system operating at the blower's typical operating power consumption of 50–80 W, the present system avoids approximately PKR 6,650–19,930 per year in electricity costs (at the 2026 NEPRA average tariff of PKR 33-40/kWh), depending on daily duty cycle. This yields a simple payback period of approximately 1.8-5.3 years on the incremental solar/battery/MPPT capital cost (PKR 35,500) relative to a grid-powered equivalent. No commercially available product combining solar-powered operation, HEPA filtration, and CO_2 absorption in a single outdoor unit was identified in the reviewed literature or commercial market. As an indicative cost anchor, grid-powered commercial units of comparable CADR (300–460 m^3/h) retail for approximately USD 100-1,000, placing the present prototype's total fabrication cost (PKR 65,193) competitively within this range despite its additional off-grid autonomy and dual-pollutant (PM2.5 + CO_2) removal capability, which was not identified among the reviewed commercial products. This estimate does not account for battery replacement (typically required every 3-5 years for sealed lead-acid batteries) or solar panel degradation over time, which should be incorporated into a full life cycle cost model in future large scale deployment studies.

Recommendations for Future Work:

The following recommendations are derived directly from the experimental findings and limitations identified in this study, rather than presented as general suggestions.

Filter housing sealing: The measured PM2.5 removal efficiency (95.6%) fell short of the H-13 filter's rated efficiency (>99.95%), a gap attributed in Section 4.6.3 to edge leakage around the filter seal. Future prototypes should incorporate foam gaskets or silicone sealant at the filter-housing interface, with pre/post seal efficiency measured directly to quantify the improvement.

Optimization of the CO_2 absorption medium: The lime-soda bed achieved a mean CO_2 removal efficiency of 59.5%, consistent with the mass-balance calculation showing that a 300 g dose provides a finite absorption capacity of 78 g CO_2 before requiring replacement. Because $Ca(OH)_2$ activity is known to decline outside its most reactive temperature range 20–50 °C and under low-humidity conditions, future work should evaluate higher-capacity or more climate-robust sorbents, such as amine-functionalized zeolites, potassium carbonate, or metal-

organic frameworks, benchmarked directly against the present 59.5% baseline and mass-balance methodology to quantify improvement.

Long-term field validation across seasons: The reported performance (95.6% PM2.5 removal, 59.5% CO_2 reduction) was measured over a five-day test window under a single set of ambient conditions. Given that Peshawar's air quality and meteorology vary substantially by season, particularly during winter temperature inversions associated with elevated AQI, extended field deployment spanning at least a full annual cycle is recommended (winter smog season, monsoon humidity, and summer peak temperatures) is recommended to confirm whether the removal efficiencies and solar-charging performance reported here are representative of sustained, real-world operation rather than a single favorable test window.

Durability testing under varying climatic conditions: The present study did not include structured environmental durability testing of the structural, filtration, or electrical subsystems. Because lime-soda reaction kinetics are temperature- and humidity-dependent and solar panel output is sensitive to temperature and soiling, future work should subject the prototype to controlled thermal cycling (covering Peshawar's full seasonal temperature range), dust-ingress testing of the blower and housing seals, and corrosion assessment of the 304 stainless-steel frame under monsoon-humidity exposure, to establish the system's operational lifespan under real deployment conditions rather than the short-term laboratory and field-test window reported here.

Secondary renewable energy integration: As solar generation alone cannot guarantee continuous operation during Peshawar's winter months, when reduced irradiance may be insufficient to fully recharge the 35 Ah battery future prototypes should evaluate a secondary source such as a vertical-axis wind turbine, benchmarked against the present system's measured recharge time and battery autonomy performance.

Smart monitoring integration: Building on the Arduino-based dual-sensor monitoring platform validated in this study, future versions should incorporate GSM/Wi-Fi connectivity for cloud-based logging and alerting, enabling integration with municipal smart-city air-quality networks as discussed in the Implications of the Study.

Commercial-scale techno-economic modeling: The preliminary techno-economic assessment presented in this study (fabrication cost, maintenance cost, and payback period for a single unit) should be extended to a life-cycle cost model incorporating battery replacement (every 3-5 years) and solar panel degradation, to evaluate the economic feasibility of multi-unit deployment across high-traffic sites in Pakistan and comparable developing countries.

References:

[1] H. Irfan, "Air pollution and cardiovascular health in South Asia: A comprehensive review," *Curr. Probl. Cardiol.*, vol. 49, no. 2, Feb. 2024, doi: 10.1016/j.cpcardiol.2023.102199.

[2] J. Wei *et al.*, "First close insight into global daily gapless 1 km PM2.5 pollution, variability, and health impact," *Nat. Commun. 2023 141*, vol. 14, no. 1, pp. 8349-, Dec. 2023, doi: 10.1038/s41467-023-43862-3.

[3] G. Gamal, N. Zanaty, and P. Nejedlik, "Long-term spatiotemporal trends and population-weighted exposure to PM2.5 in Greater Cairo (2000–2020)," *Sci. African*, vol. 31, p. e03150, Mar. 2026, doi: 10.1016/J.SCIAF.2025.E03150.

[4] J. Rentschler and N. Leonova, "Global air pollution exposure and poverty," *Nat. Commun. 2023 141*, vol. 14, no. 1, pp. 4432-, Jul. 2023, doi: 10.1038/s41467-023-39797-4.

[5] W. Batool Awan and Z. Ali, "Development of standardized PM2.5 concentration index (SPM2.5I) for monitoring and forecasting air pollution characteristics," *Theor. Appl. Climatol. 2025 15610*, vol. 156, no. 10, pp. 504-, Sep. 2025, doi: 10.1007/S00704-025-05798-0.

[6] P. Badida, A. Krishnamurthy, and J. Jayaprakash, "Meta analysis of health effects of ambient air pollution exposure in low- and middle-income countries," *Environ. Res.*, vol. 216, no. Pt 4, Jan. 2023, doi: 10.1016/j.envres.2022.114604.

[7] M. T. Nejad, K. J. Ghalehteimouri, H. Talkhabi, and Z. Dolatshahi, "The relationship between atmospheric temperature inversion and urban air pollution characteristics: a case study of Tehran, Iran," *Discov. Environ. 2023 11*, vol. 1, no. 1, pp. 17-, Oct. 2023, doi: 10.1007/S44274-023-00018-W.

[8] I. Veza, M. Z. Asy'ari, M. Idris, V. Epin, I. M. Rizwanul Fattah, and M. Spraggon, "Electric vehicle (EV) and driving towards sustainability: Comparison between EV, HEV, PHEV, and ICE vehicles to achieve net zero emissions by 2050 from EV," *Alexandria Eng. J.*, vol. 82, pp. 459–467, Nov. 2023, doi: 10.1016/j.aej.2023.10.020.

[9] M. V. Deshpande, N. Kumar, D. Pillai, V. V. Krishna, and M. Jain, "Greenhouse gas emissions from agricultural residue burning have increased by 75 % since 2011 across India," *Sci. Total Environ.*, vol. 904, p. 166944, Dec. 2023, doi: 10.1016/J.SCITOTENV.2023.166944.

[10] Q. Long, J. Ma, C. Guo, M. Wang, and Q. Wang, "High-resolution spatio-temporal estimation of street-level air pollution using mobile monitoring and machine learning," *J. Environ. Manage.*, vol. 377, Mar. 2025, doi: 10.1016/j.jenvman.2025.124642.

[11] X. Liu, M. Yang, and X. Nie, "Can city brand reduce urban air pollution? — An empirical research based on 'National Civilized City' in China," *Technol. Forecast. Soc. Change*, vol. 186, p. 122179, Jan. 2023, doi: 10.1016/J.TECHFORE.2022.122179.

[12] Z. Khanam, F. M. Sultana, and F. Mushtaq, "Environmental Pollution Control Measures and Strategies: An Overview of Recent Developments," *Geospatial Anal. Environ. Pollut. Model. Anal. Control Manag.*, pp. 385–414, Jan. 2023, doi: 10.1007/978-3-031-45300-7_15/SAVE-RESEARCH.

[13] Y. Kang, Z. X. Low, D. Zou, Z. Zhong, and W. Xing, "Multifunctional Nanofibrous Membranes for Integrated Air Purification," *Adv. Fiber Mater. 2024 65*, vol. 6, no. 5, pp. 1306–1342, May 2024, doi: 10.1007/S42765-024-00427-3.

[14] F. de A. Lima, G. B. Medeiros, P. A. M. Chagas, M. L. Aguiar, and V. G. Guerra, "Aerosol Nanoparticle Control by Electrostatic Precipitation and Filtration Processes—A Review," *Powders 2023, Vol. 2, Pages 259-298*, vol. 2, no. 2, pp. 259–298, Apr. 2023, doi: 10.3390/POWDERS2020017.

[15] Y. Xiong, J. Luo, Z. Xiao, S. Li, and X. Wang, "Scalable Cationic-Polyurea Adhesive Engineering Enabling Glass-Fiber HEPA Filters with Mechanically Robust, High-Efficiency Microbial Capture and Rapid Inactivation," *Adv. Funct. Mater.*, vol. 36, no. 52, p. e32093, Jun. 2026, doi: 10.1002/ADFM.202532093.

[16] I. P. Beckman, G. Berry, H. Cho, and G. Riveros, "Alternative High-Performance Fibers for Nonwoven HEPA Filter Media," *Aerosol Sci. Eng. 2022 71*, vol. 7, no. 1, pp. 36–58, Oct. 2022, doi: 10.1007/S41810-022-00161-6.

[17] S. Zide, H. J. Ho, L. F. Petrik, T. V. Ojumu, and A. Iizuka, "Assessment of the potential industrial applications of calcium carbonate derived from mineral carbonation of alkaline waste material," *Int. J. Environ. Sci. Technol. 2025 231*, vol. 23, no. 1, pp. 82-, Dec. 2025, doi: 10.1007/S13762-025-06922-3.

[18] "(PDF) Solar Outdoor Air Purifier with Air Quality Monitoring System." Accessed: Jul. 25, 2026. [Online]. Available: https://www.researchgate.net/publication/383631190_Solar_Outdoor_Air_Purifier_with_Air_Quality_Monitoring_System

[19] M. S. Endiz, "Design and implementation of microcontroller-based solar charge controller using modified incremental conductance MPPT algorithm," *J. Radiat. Res.*

Appl. Sci., vol. 17, no. 2, p. 100938, Jun. 2024, doi: 10.1016/J.JRRAS.2024.100938.

[20] S. Singh, P. Vishwakarma, and T. Gupta, "Review of Current and Future Indoor Air PurifyingTechnologies," *ACS ES&T Eng.*, vol. 4, no. 11, pp. 2607–2630, Nov. 2024, doi: 10.1021/ACSESTENGG.4C00460.

[21] A. Chowdhury, S. Bit, A. Majee, A. Biswas, and M. Sarkar, "Solar-Powered IoT-Based Air Quality Regulator for Indoor Air Purification," *2026 9th Int. Conf. Electron. Mater. Eng. Nano-Technology, IEMENTech 2026*, 2026, doi: 10.1109/IEMENTECH202669403.2026.11434206.

[22] K. Mhalshekar, A. Krishan, M. Gaydhane, S. Sontakke, and V. Pawar, "Advanced ElectrospunNanofibers for PhotocatalyticDegradation: Sustainable Solutions for Wastewater Remediation," *ACS Omega*, vol. 11, no. 5, pp. 6954–6985, Feb. 2026, doi: 10.1021/ACSOMEGA.5C10970.

[23] V. Anupriya, M. Selvaganesh, E. Shirley, M. Udhaya Arthi, and G. Vivitha, "Solar Boosted AI Air Cleanser for Textile Sector," *Proc. 6th Int. Conf. Inven. Res. Comput. Appl. ICIRCA 2025*, pp. 729–736, 2025, doi: 10.1109/ICIRCA65293.2025.11089845.

[24] A. Jose, C. Abraham, A. K. Soman, T. J. Ajumal, Anandakrishna, and A. Shibu, "IoT based solar powered air purifier with air quality monitoring system," *E3S Web Conf.*, vol. 529, May 2024, doi: 10.1051/E3SCONF/202452904016.

[25] B. M. Hemanth Kumar, N. Prakash, C. Namitha, H. R. Chandana, G. Jeevan, and G. Manjunath, "Solar Harmoni Air: The Integration of Solar Power for Intelligent Outdoor Air Purification and Monitoring System," *IEEE Int. Conf. Recent Adv. Sci. Eng. Technol. ICRASET 2024*, 2024, doi: 10.1109/ICRASET63057.2024.10895174.

[26] R. Yasmin, M. N. Nabi, F. Rashid, and M. A. Hossain, "Solar, Wind, Hydrogen, and Bioenergy-Based Hybrid System for Off-Grid Remote Locations: Techno-Economic and Environmental Analysis," *Clean Technol.*, vol. 7, no. 2, p. 36, Jun. 2025, doi: 10.3390/CLEANTECHNOL7020036/S1.

[27] X. Zhang, M. Zhang, Y. Cui, and Y. He, "Estimation of Daily Ground-Received Global Solar Radiation Using Air Pollutant Data," *Front. Public Heal.*, vol. 10, p. 860107, Apr. 2022, doi: 10.3389/FPUBH.2022.860107/TEXT.

[28] R. Cao *et al.*, "A Novel MethodCoupled Atomization-Bubbling Loop Interfacefor Enhanced Capture of Fly Ash Fine Particles (PM2.5):Mechanism and Removal Efficiency Modeling," *Ind. Eng. Chem. Res.*, vol. 65, no. 11, pp. 6286–6296, Mar. 2026, doi: 10.1021/ACS.IECR.5C05430.

[29] M. Xu, W. Tian, Y. Lin, Y. Xu, and J. Tao, "Development of a Compact NDIR CO2 Gas Sensor for a Portable Gas Analyzer," *Micromachines 2024, Vol. 15, Page 1203*, vol. 15, no. 10, p. 1203, Sep. 2024, doi: 10.3390/MI15101203.

[30] M. N. M. Aashiq *et al.*, "An IoT-based handheld environmental and air quality monitoring station," *Acta IMEKO*, vol. 12, no. 3, pp. 1–9, Aug. 2023, doi: 10.21014/ACTAIMEKO.V12I3.1487.

[31] "Method of Testing General Ventilation Air-Cleaning Devices for Removal Efficiency by Particle Size | Request PDF." Accessed: Aug. 02, 2026. [Online]. Available: https://www.researchgate.net/publication/332144550_Method_of_Testing_General_Ventilation_Air-Cleaning_Devices_for_Removal_Efficiency_by_Particle_Size

[32] A. Y. Mendell, S. Lee, and J. A. Siegel, "The impact of portable air cleaners on indoor particulate matter concentrations and perceptions of indoor air quality: a randomized crossover trial in three multifamily buildings," *J. Expo. Sci. Environ. Epidemiol. 2026*, pp. 1–15, Apr. 2026, doi: 10.1038/s41370-026-00894-3.

[33] A. Buonomano, C. Forzano, G. F. Giuzio, and A. Palombo, "New ventilation design criteria for energy sustainability and indoor air quality in a post Covid-19 scenario,"

Renew. Sustain. Energy Rev., vol. 182, p. 113378, Aug. 2023, doi: 10.1016/J.RSER.2023.113378.

[34] F. Parveen and S. J. Khan, "Wastewater Treatment in Pakistan: Issues, Challenges and Solutions," *Glob. Issues Water Policy*, vol. 30, pp. 323–349, 2023, doi: 10.1007/978-3-031-36131-9_12.

[35] L. Bogdanffy, C. R. Lorinţ, and A. Nicola, "Development of a Low-Cost Traffic and Air Quality Monitoring Internet of Things (IoT) System for Sustainable Urban and Environmental Management," *Sustain. 2025, Vol. 17, Page 5003*, vol. 17, no. 11, p. 5003, May 2025, doi: 10.3390/SU17115003.

[36] "Solar Panel Price in Pakistan Today August 2, 2026 - Daily Update." Accessed: Aug. 02, 2026. [Online]. Available: https://solarpanelprices.pk/

[37] "Buy castor wheels Online at Best Price in Pakistan - Daraz.pk." Accessed: Aug. 02, 2026. [Online]. Available: https://www.daraz.pk/tag/castor-wheels/

[38] "Mppt Solar Controller – Simtek Power Services." Accessed: Aug. 02, 2026. [Online]. Available: https://simtek.com.pk/product-category/mppt-solar-controller/

Copyright © by authors and 50Sea. This work is licensed under Creative Commons Attribution 4.0 International License.